International Refereed Journal of Engineering and Science (IRJES)
ISSN (Online) 2319-183X, (Print) 2319-1821
Volume 1, Issue 4(December 2012), PP.78-97
www.irjes.com

X ray cone-beam transform for algebraic reconstruction of a stratified flow inside a duct

Alberto R. F. Teixeira[1], Nilson C. Roberty[2]
[1](Nuclear Engineering Program - COPPE, Federal University of Rio de Janeiro, Brazil)
[2](Nuclear Engineering Program - COPPE, Federal University of Rio de Janeiro, Brazil)

ABSTRACT: *This work presents a methodology for reconstruction of constants by parts functions. The paper focus in one application of this methodology for identify the phases of the stratified multi-phase flow (oil-water-gas) in a duct. The principle physics is based in attenuation of X rays and Gamma rays. Each element of the composed have a specific cross-section contributing with the loss of the X rays intensity. In this study, a parallel beam for the cases of two dimension is investigated to enforce the ideas. Then, in three dimensions, each ray generates one algebraic equation. The experiment shows that with a single view it is possible obtain information of a stratified flow and reconstruct it only if there is enough number of rays transversing the medium.*

Keywords– *Inverse Problem, Multiphase flow, X ray Transform*

1. INTRODUCTION

Many industrial and medical applications involves the reconstruction of functions from a small number of views given by many function projections related with its Radon, fan beam and cone beam associated with the X or Gamma ray propagation. These functions in the reconstruction process that represents the radiation attenuation coefficients estimation are frequently associated with characteristic sub-domains inside the whole function domain. These homogeneous parts may results from the manufacture process, or from some natural stratification or segregation of components inside the body. By collecting a-priori information about the support and the value of these characteristics parts, the number of constant parameters needed to resolves the uniqueness problem of reconstruction may be reduced. In the case of parallel two dimensional X ray beam, where the projection may gives us this additional information, the procedure consists in inspect its discontinuities and back projection it accordingly. The support of the possibles parts are located inside the convex polygonal domains that result from these lines intersection. The same method may be applied for divergent beam in two or three dimensions. In this case we need to know the source position in order to back project the rays. Note that in three dimensions, the projections discontinuity determination problem is substituted by the projections images contour determination. The kind of software appropriated to implement shape from shadow X ray based support determination are based on decomposed solid geometry.

The second part of this constant by part reconstruction method is based on ray tracing. By determining the length of the intersection of a ray starting at the source and ending in the detector, we may weight the contribution of each characteristic part of the function to the detector intensity measurement. Each ray generates one algebraic equation that will compose the system with the unknown attenuation coefficients. The system may be solved with algorithms based on least square method and related regularizations procedures to infer the appropriated intensities in the support of each part of the function.

The technique of X ray attenuation is often used in the petroleum industry because of its robustness and noninvasive nature, and can perform these measurements without changing the operational conditions. The two views are arranged at an of 90 degrees to each other, the intention is to measure the attenuation of the beam that is influenced by changes in the composition of the flow. The information flows in the oil-water-gas system are usually obtained by subject interpretation from visual observations which may lead to misinterpretations. Therefore, a noninvasive system that identifies the flow regime without subjective evaluation is very important.

X and Gamma rays differ only by the nature of the source, the first is produced by interaction of accelerated electrons with a target, and the second by radioactive decay of instable isotopes such as Cesium 137 or Americium 241. The mathematics related with the interaction of these rays with the matter are the same and through this paper they will be treated as X rays. There is an enormous literature associated with the application of the methodology here developed for cross section reconstruction. Mathematical aspects of the problem are well developed and some related works that we consider important are referenced in [1; 2; 4; 5; 7; 9]. The characterization of the path of a one velocity particle in a constant by part medium can be found in [8]. In [10] we can find a study on phase volume-fraction measurement in oil-water-gas flow using fast neutrons. The

development of an X ray computed tomography system with sparse sources and domain partition can be found in [11]. The cited work [12; 13] solves this flow regime identification with the MCNP-X Monte Carlo code for experimental data syntheses and artificial neural network training. An interesting study for data processing in an experimental high-speed gamma ray experiment can be found in [14; 15] and application to the density distribution measurement in an experimental riser for cracking catalysis has been done by [16].

Since we are supposing to know only a small amount of projections, such as only one or two views, we must give more information about the support of the function. The first possibility is derive it from the analysis of the projections. Projections are X ray shadows of the cross section whose characteristic parts of the constant by parts function represents the extinction coefficient of the material. These contours can be identified by analyzing the correspondents contours inside the radiographies. In the case of one dimensional projection of the two dimensional object section, contours are discontinuities. For two dimensional projection of a three dimensional object they manifest in the radiography as curves. "Fig." 1 and 2 exemplifies the two dimensional situation. The source of the parallel beam rays used to form the projection must be consider at the ∞. We may note that the back projection of the derivative location will determines variables sized strips in which the values of the function are changing. Two or more views will make possible the determination of the convex envelop of the constants parts elements of the functions. If in addition we has some a-priori information that is independent of the projections, such as that the function represents an stratified medium as in the main application of this work, it will be easier the function support characterization.

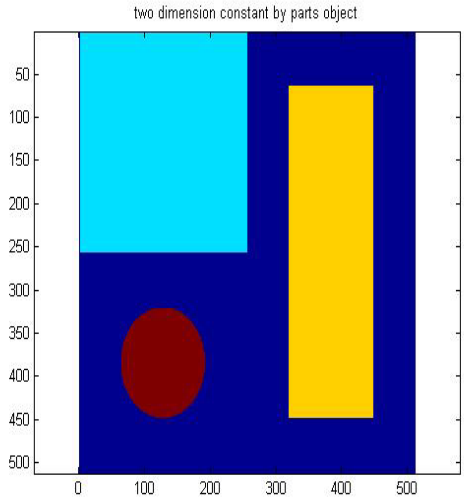

Figure 1: A Constant by parts object to be projected

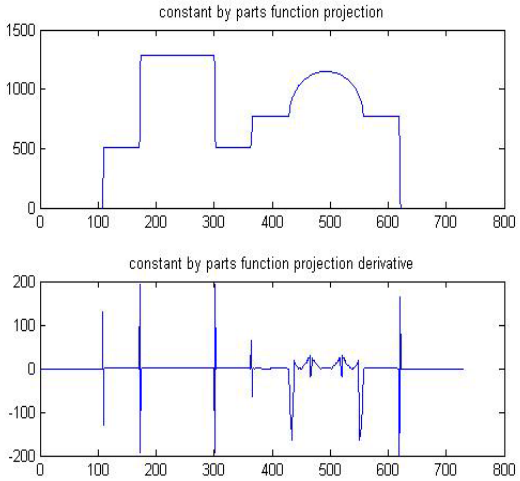

Figure 2: Projection and its derivative

1.1 The X ray attenuation model

Along a ray, the radiation can be absorbed by various known processes, depending on its nature, energy and also on the characteristics of the medium through which it propagates. There are situations in which the scattering process gives an important contribution to detectors measurements. In this case the appropriated modeling of the radiation propagation is done through the radiative transport equation. Since we are supposing ray collimation, we will neglected the scattering process and consider only the extinction process.

In this special case, the problem simplifies considerably, and the attenuation of the ray along its trajectory is exponential, and we may identify the X ray transform with the logarithm of the ray attenuation

$$\int_{\mathbb{R}^1} \sigma(\xi + t\theta)dt = -\log\left(\frac{I(E,\xi,\theta)}{I_0(E,\xi,\theta)}\right) = b(\xi,\theta) \qquad (1)$$

Where $(\xi,\theta) \in \pi_\theta X\ \mathbb{R}^{d-1}$ are, respectively, the trace of the X ray in a plane containing the $\mathbb{R}^d$ origin with normal along its direction. $I_0(E,\xi,\theta)$ is the initial source beam intensity for an specific photon with energy E that decreases along the ray trajectory to $I(E,\xi,\theta)$ in the detector position. The "Fig. 3"presents a algorithm – logarithm typical energy variation of the extinction cross section for important materials utilized in the oil-gas industry [3]. When d = 2, the X ray transform is equivalent to the Radon transform used in the Tomography. In general, we may have the parallel ray or divergent ray geometry. In our model, we are consider only a small number of views, and collecting each ray as an algebraic equation to form a system to be solved in order to reconstruction the constant by parts function representing the unknown material.

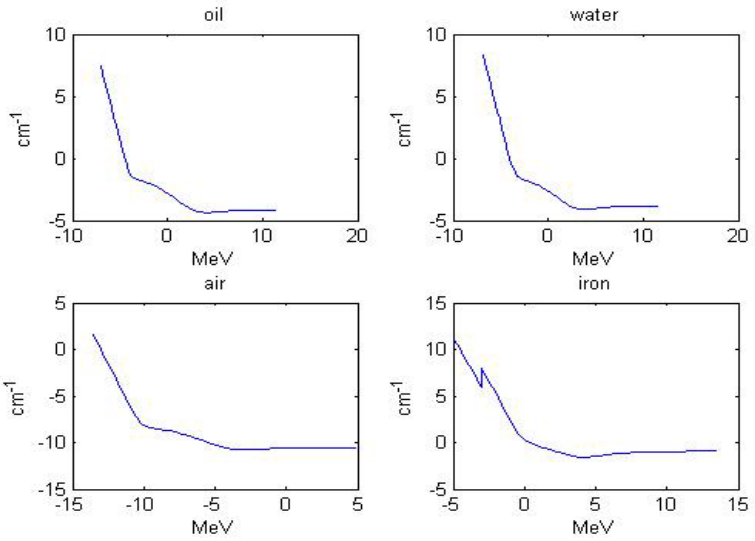

Figure 3: log-Log extinction cross section energy dependency

1.2 Mathematical aspects of divergent X ray cone beam transform

By the X ray transform for the function σ we mean

$$P[\sigma](\xi,\theta) = \int_{\mathbb{R}^1} \sigma(\xi + t\theta)dt \qquad (2)$$

where $\xi \in \mathbb{R}^d$. The divergent cone beam transform is a mapping related with equation (2) that is defined by

$$P_{\xi_d}[\sigma](\theta) = \int_0^\infty \sigma(\xi_d + t\theta)dt \qquad (3)$$

where ξ_d is the beam source position.

Theorem 1.1 Let Ω a bounded ball in $\mathbb{R}^d$. The divergent cone beam operator

$$P_{\xi_d} : L^2(\Omega) \mapsto L^2(S^{d-1}) \qquad (4)$$

Is continuous. Here $\left|\left|\xi_d\right|\right| > diam\ (\Omega)$ is supposed greater than the diameter of Ω.

Proof: First we integrate

$$|P\xi_d[\sigma](\theta)|^2 = |\int_0^\infty \sigma(\xi_d + t\theta)\, dt|^2 \leq 2\int_0^\infty |\sigma(\xi_d + t\theta)|^2 dt$$

on S^{d-1} to obtain

$$\left\|P\xi_d[\sigma]\right\|^2_{L^2(S^{d-1})} \leq 2(|\xi_d| - 1)^2 \|\sigma\|^2_{L^2(\Omega)}$$

Remark 1.1 There are one important particular situations in which the system of divergent cone beams forms a compact operator. It is when number of X rays are finite and the formed system becomes a operator with finite dimensional range [4].

We are interest in the determination of the cross section function _ in a small number of views problem. For particular situations in with this function has compact support we have the following theorem:

Theorem 1.2 Let $\Omega \subset \mathbb{R}^d$ bounded and open. Let $S \subset S^{d-1}$ open and consider Λ_d a continuously differentiable curve parametrized by $\lambda \in \mathbb{R}^1$. If:

- (i) For each θ S^{d-1}there exist an $\xi_d(\lambda) \in \Lambda_d$ such that the half-line $\xi_d(\lambda)$ + t θ, $t \geq 0$ misses Ω;
- (ii) $\sigma \in C_0^\infty(\Omega)$;
- (iii) $P_{\xi_d}[\sigma](\theta)$= 0 for $\xi_d \in \Lambda$ and $\theta \in S$

Then σ = 0 for all measured region M = $\{x = \xi_d + t\theta \in \mathbb{R}^d|_{\xi_d} \in \Lambda_d, \theta \in S\}$.

Remark 1.2 This uniqueness result tell us that three dimensional reconstruction is possible if the X ray sources Λ_d runs on a circle around the object. In fact, as we will see latter, a stratified multiphase flow inside a duct can be reconstructed with only one lateral set of data defined on a circle in a plane perpendicular to the direction of stratification. This is consequence from the fact that this small set of data can be replicated to form a full set that satisfies the conditions in this theorem.

Proof of Theorem 1.2 Since σ has compact support, we have that the moments of the cross sections function are zero in the measure region, the function itself is zero, that is,

$$\int_0^\infty t^n \sigma(\xi_d + t\theta)dt = 0, \quad \xi_d \in \Lambda, \theta \in \mathrm{S}, \ n \geq 0 \Longrightarrow \sigma = 0 \tag{5}$$

Let us define for $x = \rho\theta \in \mathbb{R}^n$

$$P\xi_{\mathrm{d}}[\sigma](x) = \int_0^\infty t^n \sigma(\xi_d + tx)\, dt = \rho^{\eta+1} \int_0^\infty t^n \sigma(\xi_d + t\theta)|dt \tag{6}$$

And proof that under the conditions of the theorem

$$P_{\xi d}^n[\sigma](x) = 0, n \geq 0, x \in M. \tag{7}$$

The proof will be conducted by induction. For n = 0, it is a consequence of (iii). Let us supposed that equation (6) is satisfied for some $n \geq 0$. The

$P_{\xi d}^n[\sigma](x) = 0, n \geq 0, x \in M.$

Let $\xi_d(\lambda)$ be a parametric representation for Λ_d. Since

$$t^{n+1} d\sigma \frac{(\xi_d(\lambda) + tx)}{d\lambda} = t^n \sum_{i=1}^{d} \frac{d\xi_d}{d\lambda} \frac{\partial\sigma}{\partial x_i}|_{\xi_d(\lambda)+tx}$$

We obtain

$$\frac{dP_{\xi_d(\lambda)}^{n+1}[\sigma](x)}{d\lambda} = \sum_{i=1}^{d} \frac{d\xi_d}{d\lambda} \frac{\partial P_{\xi_d(\lambda)}^{n+1}[\sigma](x)}{\partial x_i} = 0$$

sources Λ_d. By condition (i), for each θ, there is a source for which the X ray in direction θ misses the support of σ, and consequently, $P_{\xi_d(\lambda)}^{n+1}[\sigma](\theta) = 0$ and the induction is complete.

1.3 The Tuy's inversion formula for cone beam reconstruction

A real integrable function with three dimensional support contained in a compact set Ω can be reconstructed with a inversion formula deduced by Tuy [6] if a complete set of data when the vertex of the cone beam describes a curve Λ_d that satisfies the following conditions:

- (i) The curve is outside of the region Ω;
- (ii) the curve is bounded, continuous and almost every where differentiable;
- (iii) for all $(x, \theta) \in \Omega\, X\, S$, there exist a source in the position $\xi_d(\lambda) \in \Lambda_d$, such that $\langle \boldsymbol{x}, \theta \rangle = \langle \xi_d(\lambda), \theta \rangle$ and $\langle \xi'_d(\lambda), \theta \rangle \neq 0$, that is, for any direction θ, the plane orthogonal to θ passing through a point x ∈ Ω must cut the curve at a point $\xi_d \in \Lambda_d$ for which $\langle \xi'_d(\lambda), \theta \rangle \neq 0$.

These are the Tuy's conditions for the cone beam reconstruction. Let $\alpha = |\alpha|.\theta$ an auxiliary variable and consider the Fourier transform of the homogeneous X ray transform $\frac{1}{\alpha}P[\sigma]$ with respect to this variable

$$G(\xi, \lambda) = \int_{\mathbb{R}^3} \frac{1}{\alpha} P[\sigma](\xi_d(\lambda), \theta) \exp(-2i\pi\langle \alpha, \xi \rangle) d\alpha \tag{8}$$

Theorem 1.3 (Tuy) Supposed that the real integrable compact support function $\sigma: \Omega \subset \mathbb{R}^3 \to \mathbb{R}$ satisfies the Tuy's conditions. Then, for all x $\in \Omega$.

$$\sigma(x) = \int_0^{2\pi} \int_{\frac{-\pi}{2}}^{\frac{\pi}{2}} \frac{\cos(\phi)}{2i\pi\langle \xi'_d(\lambda), \theta\rangle} \frac{\partial G(\theta,\lambda)}{\partial \lambda} d\phi d\varphi \qquad (9)$$

The proof is a straightforward application of the Fourier transform to the derivative of (8) with respect to the curve parameter λ and can be found in (6). The main difficulty with its application is when, as we are supposing in this work, we want reconstruct the function using only a limited number of cone beam views.

1.4 The constant by part functions: X ray cone beam transform

Let us consider a compact support domain $\Omega \subset \mathbb{R}^d$; d=2,3 partitioned into disjoint open elements Ω_n; n=1,...,N in such way that:

- $\Omega = \bigcup_{n=1}^{N} \overline{\Omega_n}$;
- $\Omega_n \cap \Omega_m = 0; n, m = 1, \dots, N;$
- $\partial\Omega_n$; n=1,...,N are continuous by parts.

By the characteristics simples function associated with the element Ω_n we mean the following function:

$$\chi_n(x) = \begin{cases} 1 \; if \; x \epsilon \Omega_n \\ 0 \; if \; x \; \epsilon \; {\mathbb{R}^d}/{\Omega_n} \end{cases} \qquad (10)$$

For n=1,…,N. By a constant by parts function associated with this domain partition Ω we mean

$$\sigma(x) = \sum_{n=1}^{N} \sigma_n \chi_n(x) \qquad (11)$$

Let $x = (x_1, \dots, x_d) \epsilon \mathbb{R}^d$ and $\theta = (\cos(\theta_1), \dots, \cos(\theta_d)) \epsilon S^{d-1}$ a parametric representation of a direction in $\mathbb{R}^d$.

Let π_θ be a plane (or straight line) containing the origin in$\mathbb{R}^d$ with normal θ. Let

$$\pi_{\xi,\theta}^{\perp} = \Omega \cap \{\xi + t\theta, -\infty < t < \infty\} \neq 0 \qquad (12)$$

an straight line perpendicular to π_θ at the point $\xi \in \pi_\theta$ describing the X ray path inside Ω. Let $\sigma(x)$ the constant by parts function defined by Eq.(11) representing the medium extinction cross section. Then for each point $\xi \in \pi_\theta$and for each direction $\theta \epsilon \mathbb{R}^{d-1}$:

- There exist $\gamma_i(\xi,\theta), 0 \le i \le I(\xi,\theta)$, with $\gamma_0(\xi,\theta) < \gamma_1(\xi,\theta) < \cdots, \gamma_{I(\xi,\theta)} < \cdots < \infty$ such that the radiation path inside the this medium is given by the finite of intervals $\bigcup_{i=1}^{I(\xi,\theta)} \{\gamma_i(\xi,\theta) < s < \gamma i+1(\xi,\theta)\}$;
- And the X ray transform integral will be given by a finite sum

$$P[\sigma](\xi,\theta) = \sum_{n=1}^{N} \sigma_n \sum_{i=1}^{I(\xi,\theta)} \delta_{n,i}^{(\xi,\theta)} (\gamma_i(\xi,\theta) - \gamma_{i-1}(\xi,\theta)) \qquad (13)$$

Where

$$\delta_{n,i}^{(\xi,\theta)} = \begin{cases} 1 \; if \; \Omega_n \cap \pi_{\xi,\theta} \neq 0 \\ 0 \; if \; \Omega_n \cap \pi_{\xi,\theta} = 0 \end{cases} \qquad (14)$$

In fact, the interception of the ray with the internal boundary of the domain partition associated with the constant by part function has a finite number of traces, that is, for every $\xi \epsilon \pi_\theta$, we have define $\pi_{\xi,\theta} = \Omega \cap \{\xi + t\theta, -\infty < t < \infty\}$ and this set consit of a finite number of open intervals, i. e, there exist $\gamma_i, 0 \le i \le I$, with $\gamma_0 < \gamma_1 < \cdots, < \gamma_I$, varying with (ξ,θ), such that $\pi_{\xi,\theta} = \bigcup_{i=1}^{I} \{\xi + t\theta, \gamma_{i-1} < t < \gamma_i\}$.

Obviously, the function that gives the extinction coefficients along the ray will also be constant by parts as exemplifies in "Fig. 4".

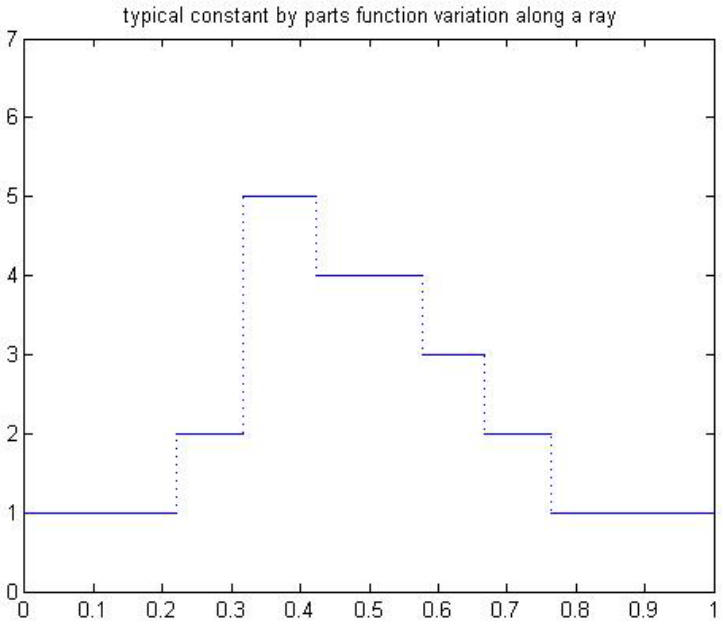

Figure 4: Typical trace of the constant by parts function along a ray

1.5 Algorithm for x ray traces determination

In order to implement the three dimensional stratified multiphase flow model inside a duct, let us consider the following stratified function in direction x3

$$\sigma(x) = \chi R_i L(x) \sum_{n=2}^{N} \sigma_n \chi_n(x_3) + \sigma_1(\chi R_e, L(x) - \chi R_i, L(x)) \quad (15)$$

where σ_0 is the extinction coefficient of the duct material, σ_n, n = 1, …, N is the same properties for the layer n material inside the duct

$$\chi R_s, L(x) = \begin{cases} 1 & if\ \sqrt{x_1^2 + x_3^2} \le R_s\ and - L \le x_2 \le +L \\ 0 & else \end{cases} \quad (16)$$

where s = e, i are respectively the external and internal radius of the duct.

$$\chi_n(x_3) = \begin{cases} 1 & if\ x_3^{n-1} \le x_3 \le x_3^n \in\ \Omega_n \\ 0 & else \end{cases} \quad (17)$$

The coordinates system origin's has been choose to be the point (0; 0; 0), as usual. The stratified layer thickness is calculated as $l_n = x_3^n - x_3^{n-1} = 2R_i/N$. By considering the X ray source position $x_s = (x_s^1, x_s^2, x_s^3)$ and detector position $x_d = (x_d^1, x_d^2, x_d^3)$ interpolation by the straight line

$$x(t) = tx_d + (1-t)x_s = tx_d^1 + (1-t)x_s^1, tx_d^2 + (1-t)x_s^2, tx_d^3 + (1-t)x_s^3, t \in [0,1] \subset \mathbb{R}^1 \quad (18)$$

Note that the X ray parameters (ξ, θ) are determined by the line x(t) linking the source detector pair. The t_i that gives the respective traces in the layers are calculated with the solution of the following problem: To find $t \in \mathbb{R}^1$ that satisfies simultaneously the system

(i) $$\left(tx_d^3 + (1-t)x_s^3\right)N/2R_i \in \mathbb{Z} \quad (19)$$

(ii) $$(tx_d^{'} + (1-t)x_s^1)^2 + \left(tx_d^3 + (1-t)x_s^3\right)^2 \le R_i^2 \quad (20)$$

(iii) $$-L \le tx_d^2 + (1-t)x_s^2 \le +L \quad (21)$$

gives by conditions (i), (ii) and (iii). The algorithm based on the solution of this system can be implemented in the following sequence of procedure:

Algorithm 1.1

1. For a pair source in position $x_s = (x_s^1, x_s^2, x_s^3)$ and detector in position $x_d = (x_d^1, x_d^2, x_d^3)$, $\theta = (\theta_1, \theta_2, \theta_3)$ is

$$\theta = \frac{(x_d^1 - x_s^1, x_d^2 - x_{s,}^2 x_d^3 - x_s^3)}{\sqrt{\sum_{i=1}^{3}(x_d^i - x_s^i)^2}} \tag{22}$$

And $\xi = (\xi_{1,}\xi_2, \xi_3)$ is solution of the equations

$$\xi_1\theta_1 + \xi_2\theta_2 + \xi_3\theta_3 = 0 \tag{23}$$

and

$$\frac{\xi_1 - x_s^1}{\sqrt{x_d^1 - x_s^1}} = \frac{\xi_2 - x_s^2}{\sqrt{x_d^2 - x_s^2}} = \frac{\xi_2 - x_s^3}{\sqrt{x_d^3 - x_s^3}} \tag{24}$$

2. For z = -N to N, calculate $t_z = \frac{\frac{2R_i z}{N} - x_s^3}{x_d^3 - x_s^3}$
3. For z = -N to N, IF $(t_z x_d^1 + (1 - t_z)x_s^1)^2 + (t_z x_d^3 + (1 - t_z)x_s^3)^2 \geq R_i^2$, discard this value t_z from the set of layers boundaries
4. Solve the following quadratic equations for t

$$(tx_d^1 + (1-t)x_s^1)^2 + (tx_d^3 + (1-t)x_s^3)^2 = R_i^2$$
$$(tx_d^1 + (1-t)x_s^1)^2 + (tx_d^3 + (1-t)x_s^3)^2 = R_e^2$$

In order to determine the X ray trace in the internal and external duct cylindrical surface,

5. If for some no discarded t_z , $\|t_z x_d^2 + (1 - t_z)x_s^2\| > L$, discard this pair source detector,
6. Also, for a pair source detector, if $\pi_{\xi,\theta}$ coincides with an interface of the layer stratification, them discard this pair.
7. The incident matrix $\delta_{n,i}^{(\xi,\theta)}$ is determined by sorting the non discarded t_z, then, n = z and I is the resulting index i(z, ξ, θ) that comes from the sorting process.
8. The trace is calculated as the distance between the interface and the source

$$\gamma_i(\xi, \theta) = \sqrt{\sum_{j=1}(x_s^j - x(t_z)^j)^2} \tag{25}$$

Figure 5 shows a representation of the a fictitious extinction cross section used in the computation of the incident matrix and the trace. This cross sections hasN = 24 stratified layers and its fictitious value is equal the parameter

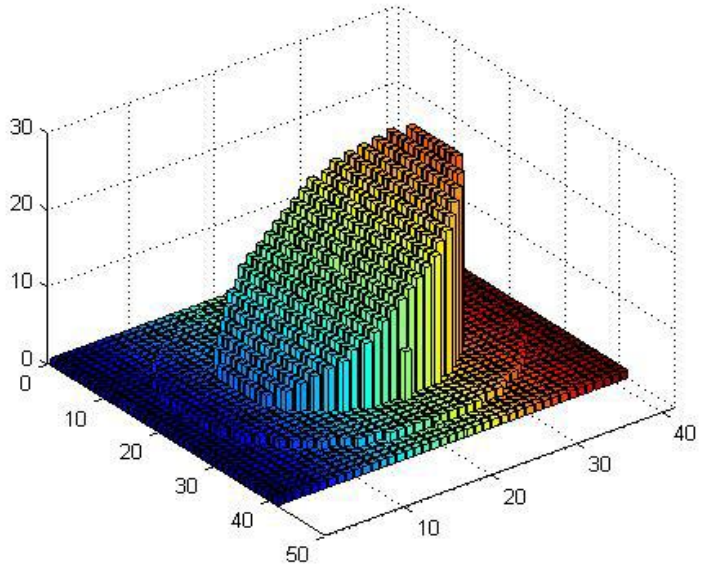

Figure 5. Weight determination

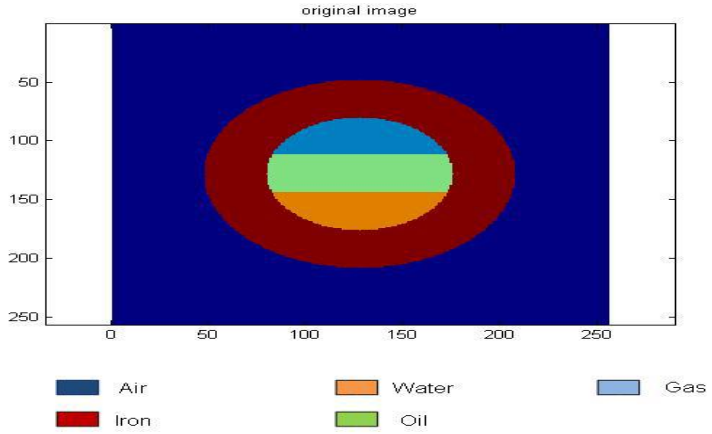

Figure 6. Oil, water and gas inside a duct

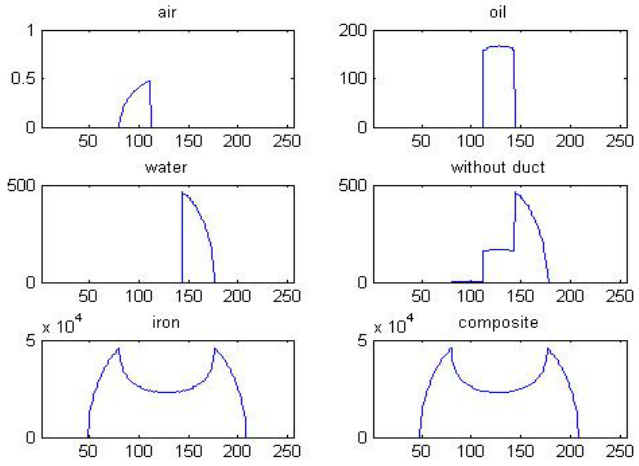

Figure 7. Optical thickness parallel beam with one view 9keV

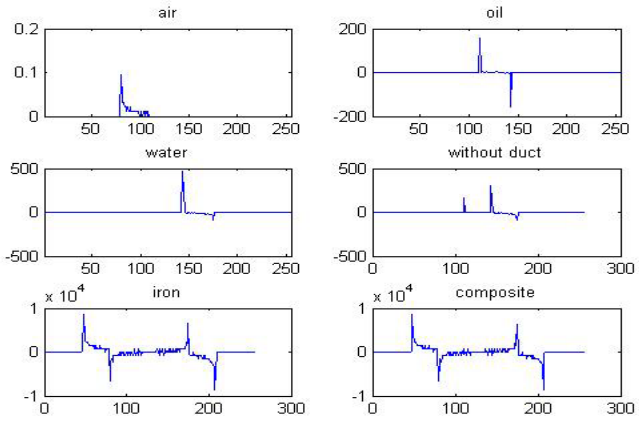

Figure 8. Derivative of optical thickness 9keV

II. MODEL GEOMETRY

We consider as an application two beams of X ray to the identification of a multiphase flow with oil, water and gas inside a metallic duct.

Due to the difference in the densities of the mixtures components, the three fluid mixture flow stratifies induced by gravity , which gives an important a-priori information about the constant by part cross section that will be reconstructed. We have used this information to model a linear system used with the reconstruction algorithm whose weight matrix parameters are determined with the algorithm 1.1.

2.1 Synthetic data generation

Numerical data has been produced with the simulated direct problem in two situations. In the first we consider only one view and collect the data in a direction parallel to the level of the flow stratification. These optical thickness are shown in ´´Fig. 7`` for energy of 9keV and ´´Fig. 9`` for one energy of 180keV. Based on the experimental three dimensional divergent beam whose geometry is showed in Fig.11, we computed the set of data with photon energy 180 KeV showed in Fig. 12 for the first source position 1.

These data are used to test our methodology for identification of the interface between the three phases of fluid inside the duct. We proceed the synthetization of the data by calculating the integral in equation (2) with a prescribed three phase constant by parts distribution of extinction cross section.

The position of source detector pair are respectively, $\{(x_s^{(j)},x_d^{(d)})\}$; j=1,2} = {((0,0,64),(-16*8 : 8 : 16*8, -16*8 : 8 : 16*8 ,-64)) ; ((64,0,0), (-64, -16*8 : 8 : 16*8, -16*8 : 8 : 16*8))} for the case of 2 * 429 rays crossing the duct, and $\{(x_s^{(j)},x_d^{(d)})\}$; j=1,2} = {((0,0,64), (-8*8 : 4 : 8*8,-8*8 : 4 : 8*8, -64)) ; ((64,0,0), (-64, -8*8 : 4 : 8*8, -8*8 : 4 : 8*8))} for the case of 2* 825 rays crossing the duct, which corresponds to two sets with two groups of divergent beams data with source rotated by $\pi/2$. The duct axis in the direction x_2, as shown schematically in Fig.(11). The external and internal pipe radius are respectively, 36 and 24 and the x_3 level of water and air are -10 and 10, respectively. The oil layer is situated between these two level.

For each source the set of detector positions distributed in a plane tangent the cylinder with radius 64 and axis equal x_2 collects the values of X ray integral along these pairs of directions. These kind of data are known in the literature as the optical thickness between the source and the detector and a typical distribution of the data synthesized in this work is shown in Fig. 12. The related experiments investigated will be named, the lateral and top experiments for the 429 and 825 rays per view cases.

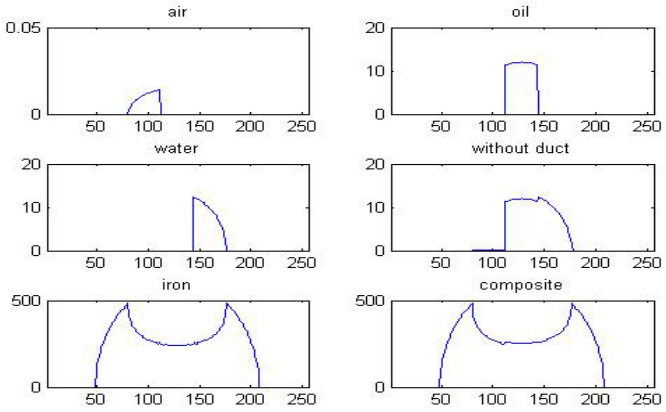

Figure 9. Parallel beam on view 180keV

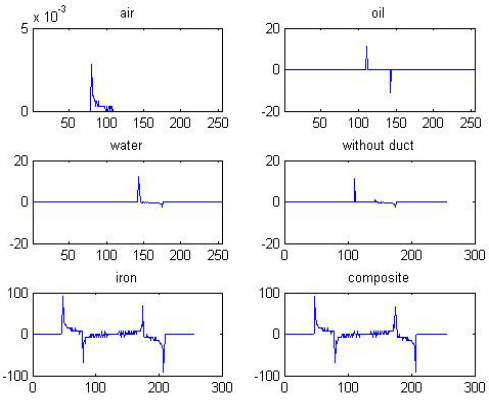

Figure 10. Derivative parallel beam optical thickness 180keV.

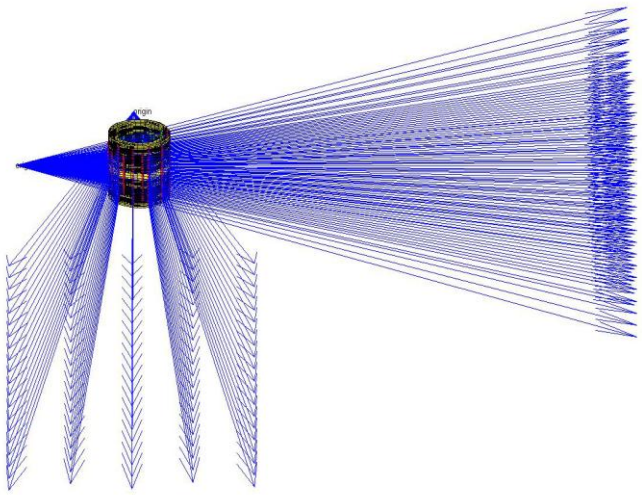

Figure 11. Divergent beam experiment set

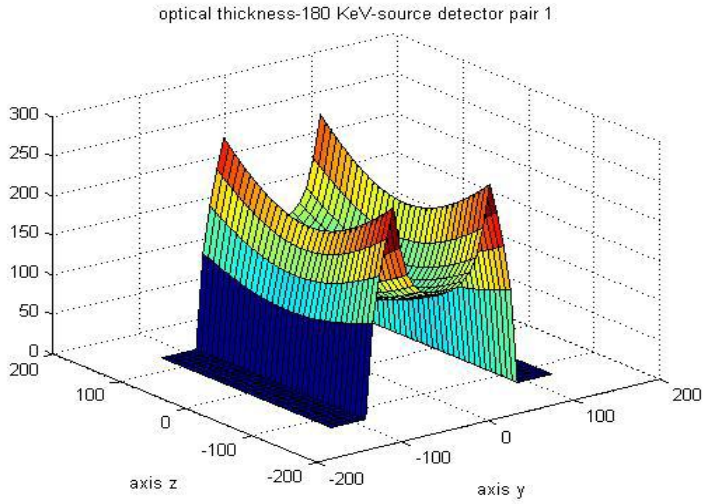

Figure 12. Optical thickness for the source position 1 – 180keV

III. ALGEBRAIC PROBLEM FORMULATION

For a radiation energy E fixed, let us consider the following problem: Giving some set of data {b(ξ, θ), ξ and θ associated with a set of rays} to find the constant by part function σ solution to the system formed with the respective associated X ray optical thickness Eq.(1). By using the a-priori information about the support of the function that represents the cross section to be reconstructed, our problem becomes the following linear algebraic system problem.

Problem 3.1 (Algebraic Linear System)

For a set of rays associated with (ξ, θ), given: {b(ξ, θ)}, $\delta_{i(\xi,\theta)}$ and $\gamma_{i(\xi,\theta)}$, i=1,…,I(ξ, θ), to find σ_n such that:

$$\sum_{n=1}^{N} \sum_{i=1}^{I(\xi,\theta)} \sigma_n \delta_{n,i(\xi,\theta)} (\gamma_{i(\xi,\theta)} - \gamma_{i(\xi,\theta)-1}) = \text{b}(\xi, \theta) \quad (26)$$

IV. LINEAR SYSTEM INVERSION

Let us give a matrix representation to the problem by defining

$$A^{n}_{(\xi,\theta)} = \sum_{i=1}^{I(\xi,\theta)} \delta_{n,i(\xi,\theta)} (\gamma_{i(\xi,\theta)} - \gamma_{i(\xi,\theta)-1}) \quad (27)$$

And write the problem as.

Problem 4.1 (Algebraic Linear System) Fixed the photon energy E, for a set of rays associated with (ξ, θ), given $b(\xi, \theta)$, to find σ_n such that:

$$\sum_{n=1}^{N} A^n_{(\xi,\theta)}\, \sigma_n = b(\xi, \theta) \tag{28}$$

The physical system modeled by Eq.(1) when a discrete number of X rays attenuations are measured constitutes an inverse problem with [4] whose theory has been extensively studied and constitutes an main chapter in the inverse problem subject. The system given by Eq.(28), in which the consequences of the stratification in the model has been introduced, can have repeated lines and can be singular if not enough lines cross the domain of the function to be reconstructed or if they cross in an inappropriate angle of incidence.

The remotion of repeated lines of this system can be easily done but has been noted to have no influence the solution. Fig. 13 and Fig. 14 shows the singular values of the weight matrix to be used in the reconstruction for the problem with 2 * 429 rays with top and lateral views. Note that this problem presents singular behavior and has an ill-determined rank that does not change if we removes the repeated lines. Fig. 15 and Fig. 16 shows the singular values of the weight matrix for problems with 825 rays in one lateral view. Note that the non singular behavior of the lateral weight matrix in contrast with the high singular behavior of the top view matrix. Fig. 17,for another hand, shows that the singular values of the weight matrix for lateral view when the number of rays crossing the duct are not enough for reconstruction with only one view, even if it is a lateral one.

The singularity presents in the problem is associated with the compacticity of the X ray operator has been removed by the adoption of the constant by parts representation to cross sections, and the singular behavior that remains is due to data incompleteness. Techniques based on singular values truncation may be adopted when the system is not so big, which is the case of the present work.

4.1 The regularization problem

Through the inverse of a linear system can be constructed by using the Moore-Penrose pseudo inverse, for which non existence and non uniqueness are removed by least squares projection of the data in the operator range and factorization of indeterminate solutions due to non trivial operator null, respectively, when the operator presents compactness, such as the observed in the present 3D X ray transform based system, the operator range is not closed and the problem presents instability in the presence of numerical or experimental noise. The most common techniques that are adopted to solve these kind of problem are the singular value decomposition method, also known as spectral cutoff, the Tikhonov regularization method, which is a kind of optimization penalized by the noise level and the Landweber iterative method associated with some discrepancy based stopping rule. All these methodology are fundamentally based on the idea that the unstably problem must be substituted by an problem that will give an stable but approximated solution to the original problem. The error is committed with noise level that the original problem presents and the higher the noise level the worst the approximation will expected to be. The relation between the original and the approximated problem is controlled by a small parameter ε, which acquires different meaning, depending on the regularization method that we are using, but that is always related with the noise to signal ratio associated with the data been used.

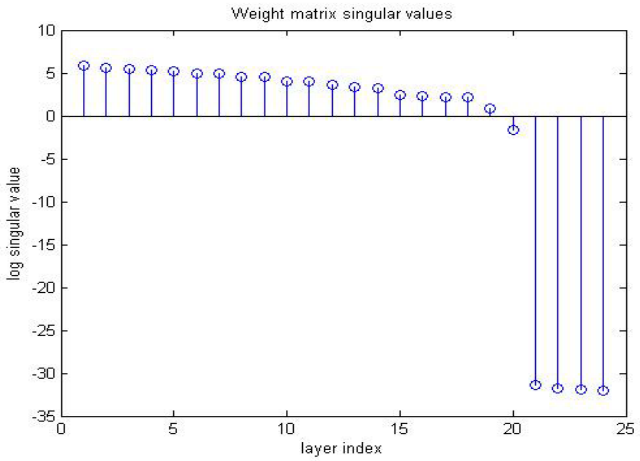

Figure 13. weight marix singular values decomposition

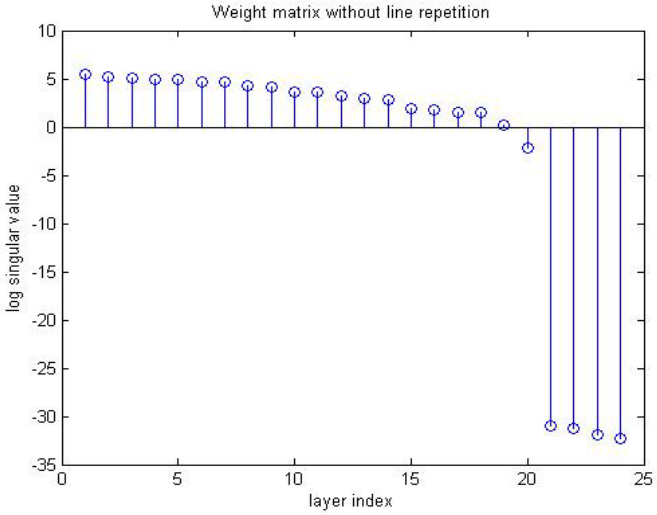

Figure 14. weight marix singular values decomposition with repited line exclusion

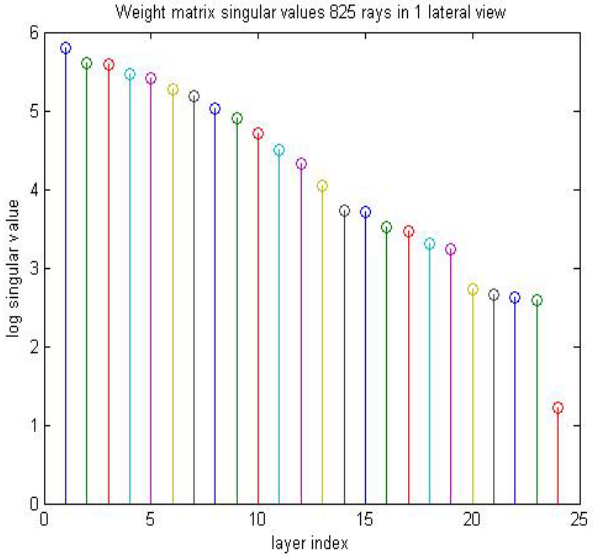

Figure 15. weight marix singular values decomposition for 1 lateral view with 825vrays

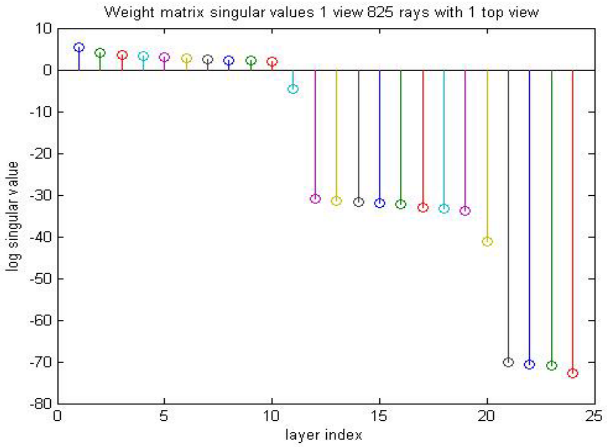

Figure 16. weight marix singular values decomposition for 1top view with 825vrays

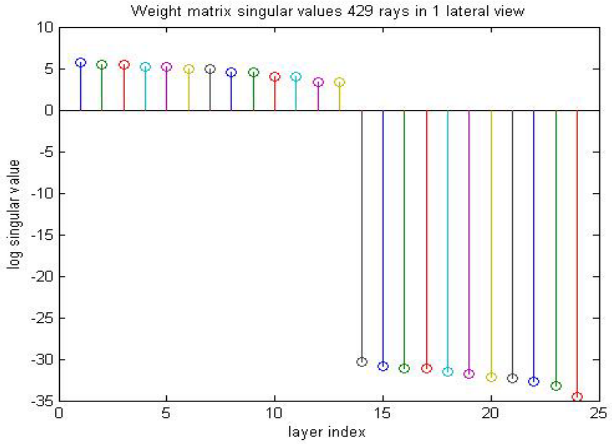

Figure 17. weight marix singular values decomposition for 1top view with 429vrays

4.2 The singular value decomposition method

The singular value decomposition method is a standard linear algebra procedure to find the decomposition of matrix $A = VDU^T$ in system (28). The matrices **V** and **U** are orthonormal and forms a basis for, respectively, the domain and the range of the matrix (operator) **A**, that is, they are square matrices with size equal the number of lines (m) and columns (n) of **A**, respectively. On other hand, the matrix **D** is a diagonal n X m matrix whose entries are the singular values of matrix **A**. The main idea in the SVD regularization method is constructed the regularized pseudo inverse:

$$\mathcal{X}_\varepsilon^\dagger = A_\varepsilon^\dagger b \tag{29}$$

Where

$$A_\varepsilon^\dagger = UD_\varepsilon^\dagger V^T \tag{30}$$

and $D_\varepsilon^\dagger$ is an diagonal n X matrix with inverse entries of the diagonal m X n matrix D truncated by the rule $\mu^2 \leq \epsilon(\delta)$. When the squared singular value μ^2 becomes less than the parameter ϵ which is of the same order of the noise level δ, this value is not invert and is ruled as zero in the inverse. Fig. 18 and Fig.19 shows multiphase flow interface and cross sections values for the case with one lateral view and 825 X rays for noise levels 1% and 5%, respectively. In this case in which the angle and the number of rays are adequetely, no cutoff is necessary and the reconstruction is straightforward. In order to consider a case in which the regularization will be necessary, let us consider the problem with two views from top and lateral, but with insufficient numbers of rays. It is not difficult to see from the svd plot shown in Fig. 13 and Fig. 14 that the appropriated cutoff for this problem is μ = 0.1, 0.3 and 3.0.

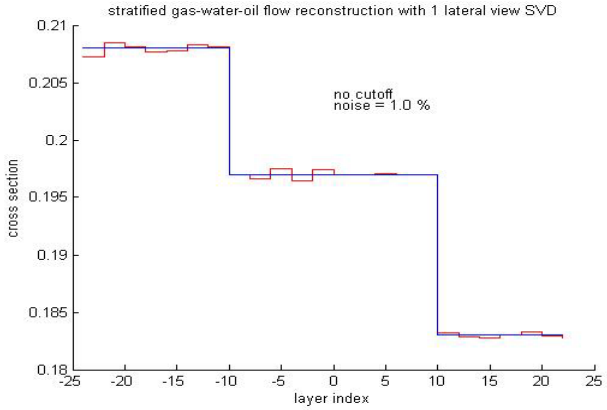

Figure 18. SVD cross section reconstruction for 1 lateral view with 1% noise.

Figure 20 shows a good reconstruction in red, as compared to the exact cross section in blue that start to becomes worst in Fig. 21 for 0.5% noise level and becomes unaccetable as a adequated reconstruction for a not so higher noise level equal to 1.0% in Fig. 22 for the cutoff at .1. We then follows increasing the cutoff

value to accomplish with higher levels of noise. Figures 23 and 24 show that the cutoff at .3 gives goods reconstructions for higher noise levels as 1.0% and 2.0%, but for the higher noise level of 5.0%. Figures 25 and 26, we can not obtain results of the same quality for both cutoff points 0.3 and 3.0.

Note that is a common sense in the singular value decomposition regularization method that by truncation we means the removal of the higher frequencies components of the representation of the solution by neglecting the small singular values and doing the pseudo inversion without them. We must understanding the meaning of small singular values are relatives between then, that is, in this model problem the higher singular value is 328.627, so values of the order 0.1 , 0.3 and 3.0 are relatively small and can be neglected. Obviously, in case that we are working with matrices with norm equal 1, that is , dividing then by its greater singular value, these cutoff points will be numbers smaller than 1:0 as expected.

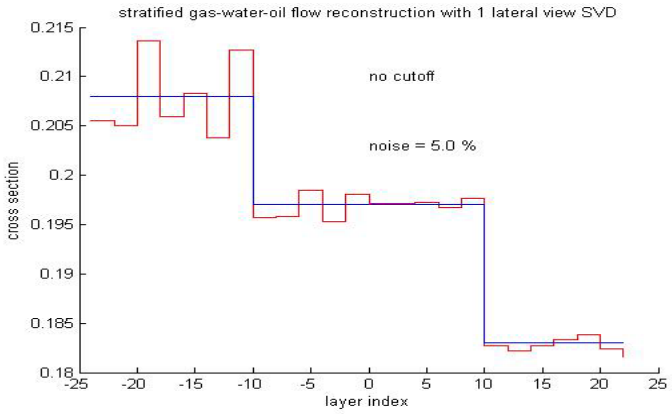

Figure 19. SVD cross section reconstruction for 1 lateral view with 5% noise.

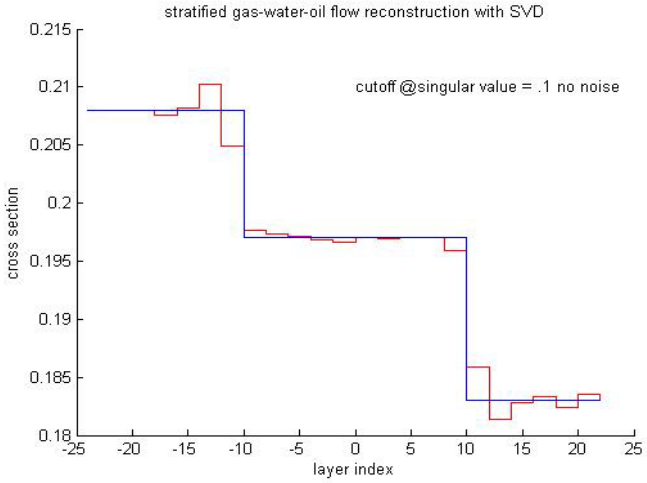

Figure 20. SVD cross section reconstruction for data without noise

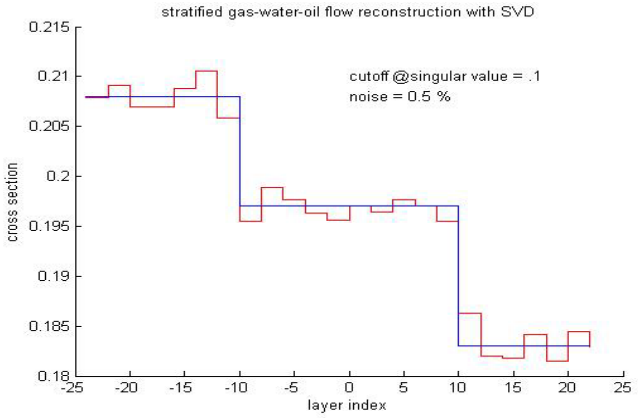

Figure 21. SVD cross section reconstruction for data with 0.5% noise

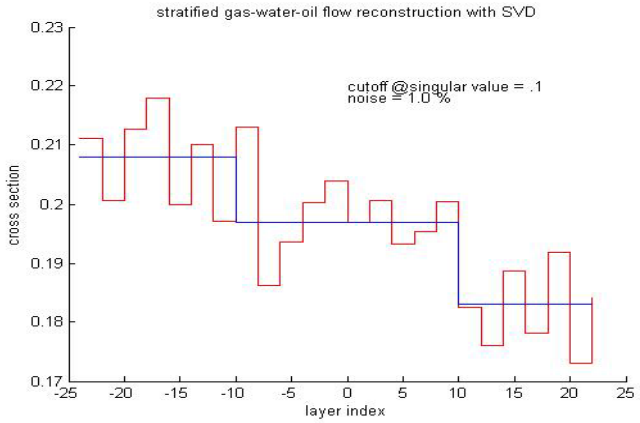

Figure 22. SVD cross section reconstruction for data with 1.0% noise

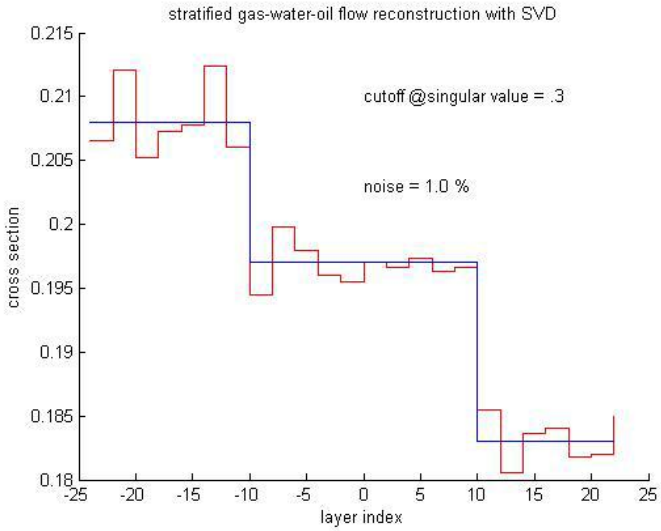

Figure 23. SVD cross section reconstruction with cutoff at .3 for data with 1.0% noise

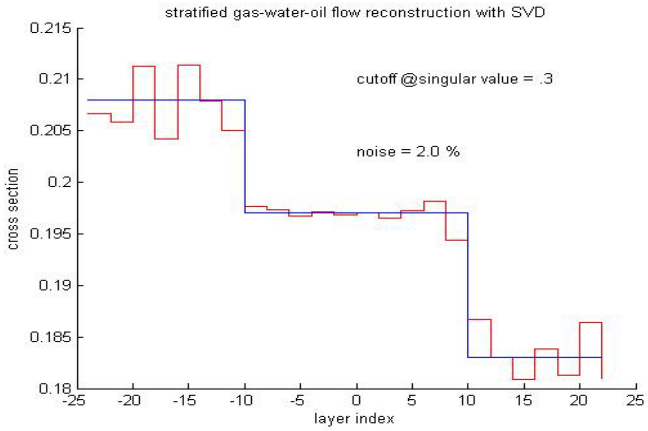

Figure 24. SVD cross section reconstruction with cutoff at .3 for data with 2.0% noise

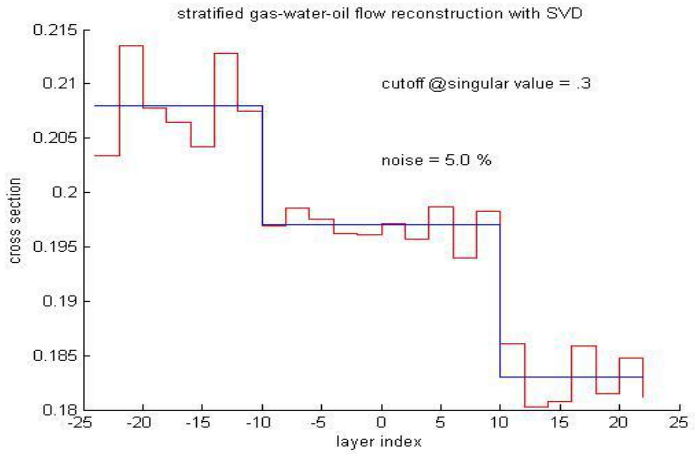

Figure 25. SVD cross section reconstruction with cutoff at .3 for data with 2.0% noise

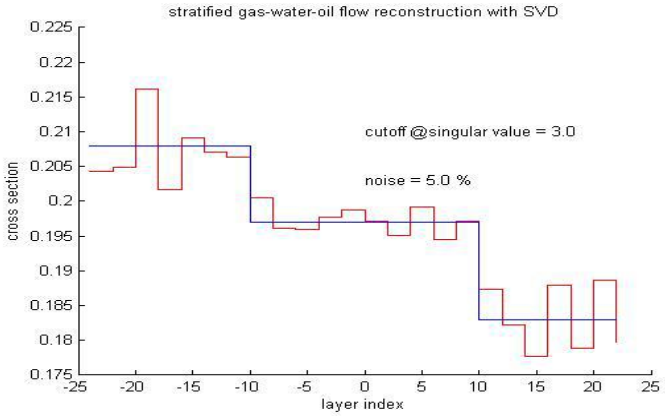

Figure 26. SVD cross section reconstruction with cutoff at .3 for data with 5.0% noise

4.3 The Tikhonov regularization method

We again consider the top and laterals views in the 2 X 429 rays problem in order to investigate the application of the Tikhonov regularization method, which is based on the following optimization problem:

Problem 4.2 (**Tikhonov regularization problem**) Fixed the photon energy E, for a set of rays associated with (ξ, θ), to find the extinction coefficient **x** which is solution of the following minimization problem

$$\text{Min}\{||Ax - b||^2 + \epsilon||x||^2\} \quad (31)$$

The parameter ϵ is the Tikhonov regularization parameter (noise to signal ratio) and is choose in a such way that the error due to modification of the original problem doesn't compromises the stabilities benefits introduced by the improvement of the numerical condition number of the algebraic matrices problem.For small size systems such that given by the X ray transform Eq. (26), the solution can also be written formally with Eq. (29 and 30), but the diagonalized Tikhonov regularized pseudo inverse $D_{\mathcal{E}}^{\dagger}$ is an diagonal n X m matrix with entries $\lambda_{\epsilon} \frac{\mu}{\mu^2+\epsilon}$.

4.4 The L curve method to the noise to signal parameter ε best determination

The L curve method for determination of the best regularization parameter ϵ for the Tikhonov solution $x_{\epsilon,\delta}^{\dagger}$ when noised data b^{δ} are not known exactly but with within the noise level $\|b - b^{\delta}\| \leq \delta$ is based on the monotonicity of the curvature of the the following curve

$$\epsilon > 0 \mapsto \big(f(\epsilon), g(\epsilon)\big) \coloneqq (||Ax_{\epsilon,\delta}^{\dagger} - b^{\delta}||^2, ||x_{\epsilon,\delta}^{\dagger}||^2) \quad (32)$$

relating the norm of residual in the data space and the norm of the pseudo inverse in the signal space. Following [9], in the case of small size systems we can use SVD to express these quantities in terms of the singular values:

$$\left|\left|Ax_{\epsilon,\delta}^{\dagger} - b^{\delta}\right|\right|^2 = \sum_{i=1}^{N} \frac{\epsilon^2}{(\mu_i^2+\epsilon)^2} |v_i^T b^{\delta}|^2 \quad (33)$$

$$||x_{\epsilon,\delta}^{\dagger}||^2 = \sum_{i=1}^{N} \frac{\mu_i^2}{(\mu_i^2+\epsilon)^2} |v_i^T b^{\delta}|^2 \quad (34)$$

The complete range of regularizations parameter $1 \geq \epsilon \geq 6{,}2506\, e-11$ practically do not influence the reconstructions for the no noise data case. The stably reconstruction at the ϵ parameter lower bound 6,25066 e-11 is slight better than the other reconstruction. For a lower ϵ =3,7276 e-11 the reconstruction became instable and the its unacceptably result is shows in Fig. 31. The Tikhonov regularization in presence of noise of 0.005% L curve in the range $1{,}7783 \geq \epsilon \geq 0{,}56234$ is shown in Fig. 32. A related flow interface and cross section reconstruction are presented in Fig. 33. These results shows the inadequacy of the Tikhonov regularization method in presence of noise. The justification is that the weight matrix rank is not ill-determined with singular values decaing smoothly toward zero. As the SVD decomposition has shown, this problem becames rank deficient when the nunber of rays are not sufficient to well posed the problem.

V. CONCLUSIONS

The interface and cross sections values associated with the three phase stratified flow (oil-water-gas) can be reconstructed with only one lateral view if a sufficiently number of X rays is provide. The experiments presents had shown that the hypotheses of constant by parts cross section adopted in the model is enough to resolved the compactness issue that frequently generates ill-posed rank discrete problems. So, the problem becomes rank deficient only when insufficient data are provides. If this is not the case, the reconstruction for noised data can be conducted with conventional linear algebra solvers.

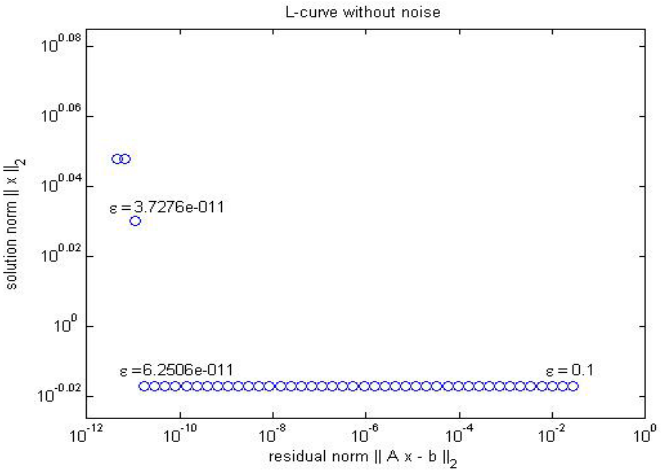

Figure 27. L curve Tikhonov regularization for data without noise

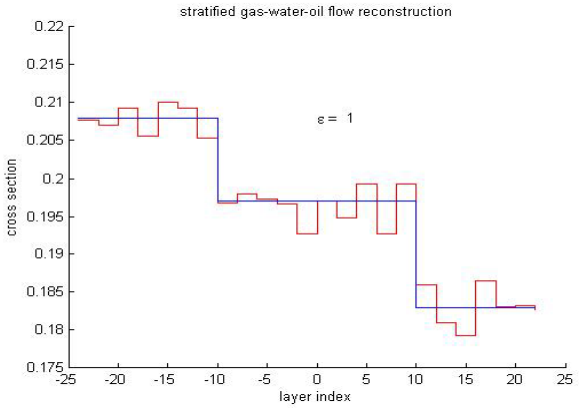

Figura 28. Cross section reconstruction by Tikhonov method for ε = 1

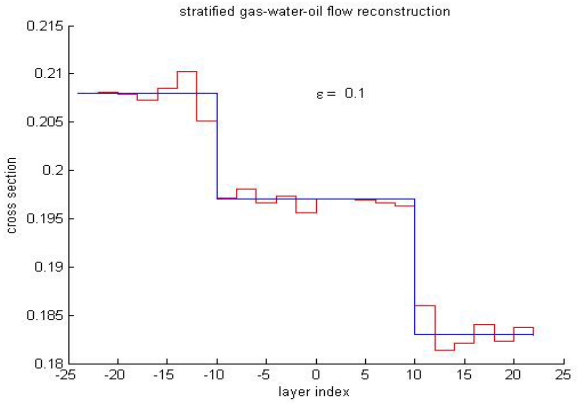

Figura 29. Cross section reconstruction by Tikhonov method for ε = .1

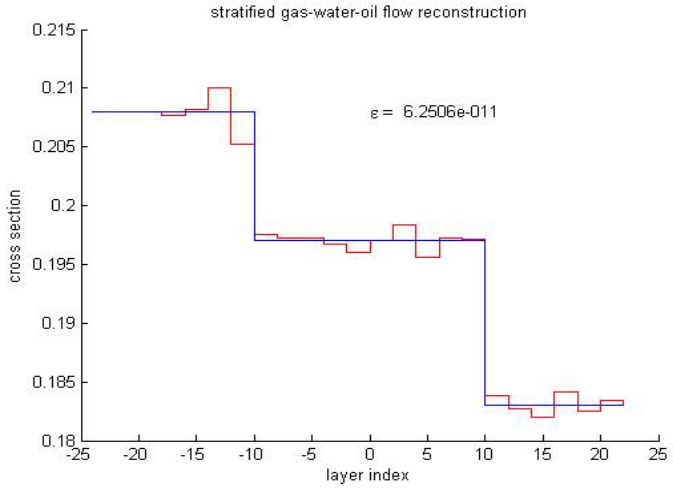

Figura 30. Cross section reconstruction by Tikhonov method under at L curve knee

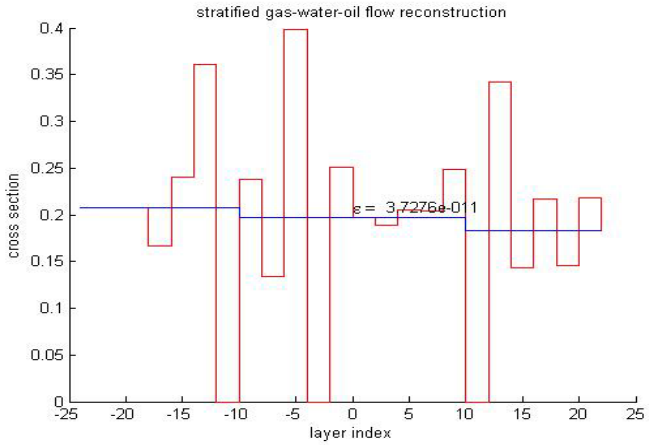

Figure 31. Cross section reconstruction by Tikhonov method under at L curve knee

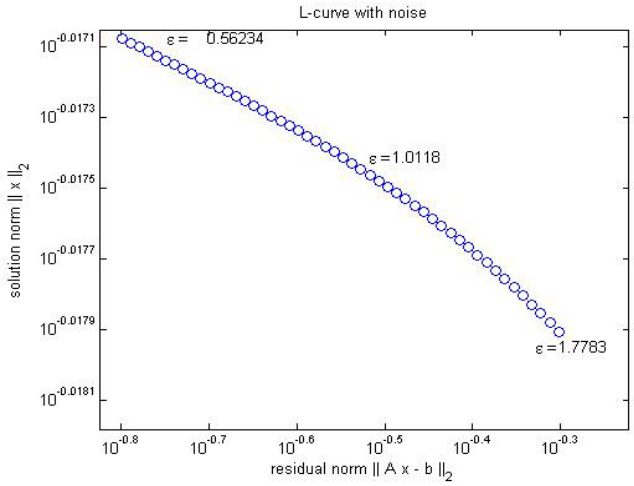

Figure 32. l curve for Tikhonov regularization for data with 0.5% noise

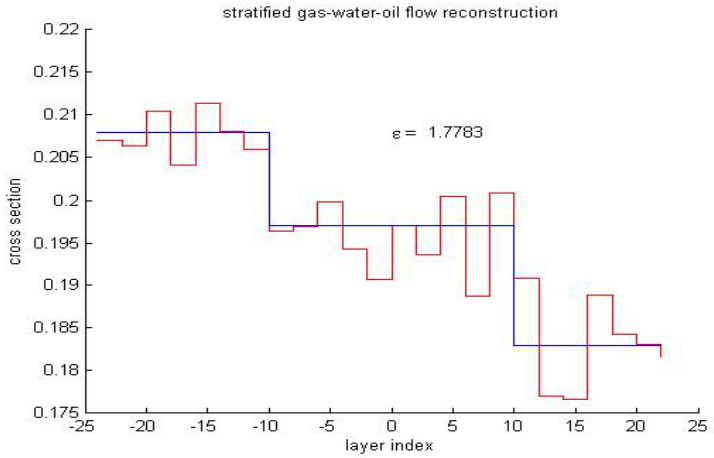

Figure 33. Cross section reconstruction by Tikhonov method with 0.5% noise with ε = 1.7783

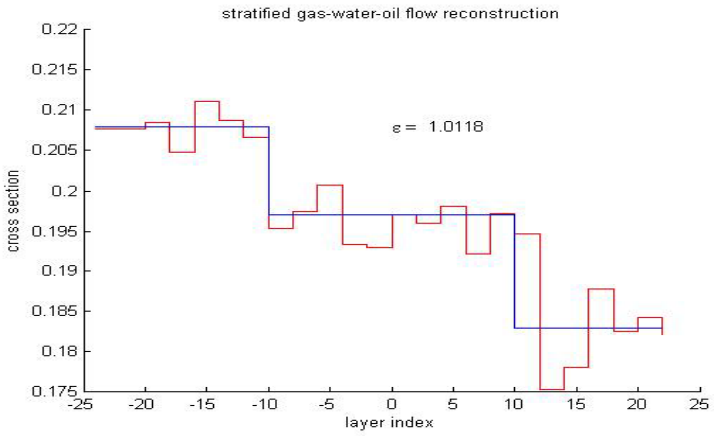

Figure 34. Cross section reconstruction by Tikhonov method with 0.5% noise with ε = 1.0118

REFERENCES

[1] Engl, H. W.,Hanke, M. and Neubauer, A. ,"Regularization of Inverse problems", Mathematics and its Applications, Vol 375, Kluwer Academic Publlishers, 2000.

[2] Hansen, P. C., 1998, "Rank-Deficient and Discrete I11-Posed Problem", ISBN 0-89871-403-6.

[3] Hubbell,J. H. and Seltzer, S. M., "Tables of X-Ray Mass Attenuation Coefficients and Mass Energy-Absorption Coefficients from 1 keV to 20 MeV for Elements Z = 1 to 92 and 48 Additional Substances of Dosimetric Interest", http://www.nist.gov/physlab/data/xraycoef, 1996.

[4] Bertero M., De Mol C. and Pikes E. R., "Linear inverse problems with discrete data: II. Stability and regularisation", Inverse Problems, 4 (1988) 573-594.

[5] Kak, A. C. and Slanley, M., "Principles of Computerized Tomographic Imaging", IEEE Press, New York,1987.

[6] Tuy, H. K., "An inversion formula for cone-beam reconstruction", Siam J. Appl. Math, Vol 43, No 3, June(1983) 546-552.

[7] Natterer, F. and Wubbeling, F., "Mathematical methods in Image Reconstruction", Siam Monographs onMathematical Modeling and Computation, 2001.

[8] Kaper, G. H., Leaf, G. K. and Linderman, A. J., 1975, "Formulation of a Ritz-Garlekin type procedure for the approximate solution of the neutron transport equation", Journal of Mathematical Analysis and Applications, Vol. 50, pp.42-65.

[9] Engl H. W. and Grever W.,"Using the L curve for determining optimal regularization parameters", Numer Math, 69; 25-31 (1994).

[10] Hussein, E. M. A. and Han, P., 1995, "Phase volume-fraction measurement in oil-water-gas flow using fast neutrons", Nuclear Geophysis, Vol.9, pp. 229-234149-167.

[11] Hu, B. et.al.,2005, "Development of an X ray computed tomography (CT) system with sparse sources: application to three-phase pipe flow visualization", Experiments in fluids, Vol. 39, pp.667-678.

[12] Salgado, C. M., Schirru, R., Brando, L. E. B. and Pereira, M. N. A., 2009, "Flow regime identification with MCNP-X Code and artificial neural network", Proceedings of the 2009 International Nuclear Atlantic Conference-INAC 2009, ABEN, Rio de Janeiro, Brazil, ISBN: 978-85-99141-03-8.

[13] Salgado, C. M., Brando, L. E. B., Pereira, C. M. N., Ramos, R., Silva, A. X. and Schirru, R., "Prediction of volume fractions in three-phase flows using nuclear technique and artificial neural network", Applied Radiation and Isotopes, doi:10.1016/j.apradiso.2009.02.093-Reference ARI4470(2009).

[14] Froystein,T., Kvandal, H. and Aakre, H., 2005, "Dual energy gamma tomography system for high pressure multiphase flow",Flow Measurement and Instrumentation, Vol. 16, pp. 99-112.

[15] Maad, R. and Johansen, G. A., "Experimental analysis of high-speed gamma-ray tomography performance", Meas. Sci. Technol. 19 (2008) 085502

[16] Dantas, C. C. et all., " Measurement of density distribution of a cracking catalysis in experimental riser with a sampling procedure for gamma ray tomography", Nuclear Instruments and Methods in Physics Research B 266 (2008), pp 841-848